ELSEVIER

Biophysical Chemistry 66 (1997) 1–12

Biophysical Chemistry

Physico-chemical properties of the heat-induced 'superaggregates' of amphotericin B

François Gaboriau *, Monique Chéron, Liliane Leroy, Jacques Bolard

Laboratoire de Physicochimie Biomoléculaire et Cellulaire (CNRS UA 2056), Université Pierre et Marie Curie, case 138, 4 place Jussieu, 75252 Paris cedex 05, France

Received 7 May 1996; accepted 3 September 1996

Abstract

The aggregation state of amphotericin B (AmB) was previously reported to modulate its therapeutic efficiency. As a preliminary study to test the biological effects of 'superaggregates' generated by heat treatment, we present spectroscopic data related to their formation in aqueous solutions. Drastic changes in the AmB aggregation state in water were shown to occur on heating at 50–60 °C. The concentration of the aggregates formed at high (A_t) or room (A) temperature, and the concentration of the monomeric form (M) of AmB were calculated by processing absorption data. The thermally induced conversion from A to A_t depends on the AmB concentration. Rayleigh scattering measurements suggest that the A_t aggregates are larger than the A aggregates. At room temperature, the condensation rate of A with M—leading to the 'superaggregated' form A_t—was slower and depended on the concentration of M. The superaggregated species A_t was shown to be the most chemically stable species. Physico-chemical properties of these superaggregates are discussed as a potential new solution to improve the therapeutic efficacy of AmB.

Keywords: Amphotericin B; Drug delivery; Aggregation; Absorption; Circular dichroism; Auto-oxidation

1. Introduction

Amphotericin B (AmB) is a heptaene macrolide antibiotic that exhibits antifungal activity. Despite its various side-effects, including nephrotoxicity, hemolytic anemia and electrolyte abnormalities, Fungizone®—the commercial form of AmB—remains the most widely used drug to treat deep-seated mycotic infections. The increased frequency of opportunistic fungal infections, which is related to the increased frequency of organ transplants and to the spread of acquired immunodeficiency syndrome (AIDS), explains the large number of studies undertaken since the mid-1980s to improve the therapeutic efficacy towards fungal cells and to reduce the cytotoxicity of this drug on mammalian cells (for reviews, see the work of Bolard and Brajtburg [1,2]).

The aggregation state of AmB was reported to depend on various parameters [3–12]. Previous studies showed that the selectivity of AmB also depends on its aggregation state [5,10,12,13]. The selectivity of the AmB activity against ergosterol-containing

Abbreviations: RBCs, Red blood cells; CD, Circular dichroism; AmB, Amphotericin B; DMSO, Dimethylsulfoxide; DMF, Dimethylformamide; EPC, Egg phosphatidyl choline; LUV, Large unilamellar vesicles

* Corresponding author.

PII S0301-4622(96)02241-7

fungal cells with respect to the toxicity against cholesterol-containing mammalian cells can be increased by using liposomal formulations [14–20].

In aqueous solution, AmB is present as a mixture of various species in equilibrium: monomers (M), and soluble and insoluble aggregates. The concentrations of each species depend not only on the total AmB concentration but also on the method of preparing the solutions [12]. The concentration of the AmB stock solutions was also reported to modify the relative proportion of each species [12]. It was concluded that the self-associated soluble form of AmB and the monomers induce K^+ permeability more efficiently in cholesterol-containing membranes than do insoluble aggregates [21]. Only self-associated AmB was shown to increase the K^+ permeability of cholesterol-containing egg phosphatidyl choline (EPC) vesicles, while both monomeric and aggregated AmB modify the K^+ permeability in ergosterol-containing liposomes [13]. Moreover, the toxic and chemotherapeutic effects were previously demonstrated to be correlated with the particle size of intravenously injected amphotericin B [22]. The particle size also affects the antibiotic inhibitory effect on lymphocyte chemotaxis [23]. From these results, it appears that the best strategy to decrease the cytotoxicity of AmB is to develop new derivatives and/or formulations that lead to decreased aggregation, or to less toxic aggregates.

The equilibrium between monomers and aggregates appears to play a key role in drug activity. Consequently, the structural study and quantification of the aggregates constitute essential steps in the understanding of the molecular mechanisms of this antifungal agent with respect to both selectivity and cytotoxicity. Heat treatment was reported to increase the size of AmB aggregates [24]. In a first attempt to test the biological effects of 'superaggregates' generated by heat treatment, we present spectroscopic data on the formation of superaggregates in aqueous solution. We developed a simple method to quantify the concentrations of each species, by processing absorption data. This algorithm was used to estimate the quantities of each species in aqueous solutions as a function of various experimental factors, such as the concentrations of the stock and final diluted solutions, as well as the temperature.

Reactive oxygen species generated by this polyenic antibiotic have been assumed to be involved in its auto-oxidative degradation [25] and in its peroxidative activity at the membrane level, which could partly explain AmB's cytotoxicity [26]. It was suggested that the AmB aggregation state modulates the AmB auto-oxidation kinetics [27,28]. Here, the stability of the various aggregated species was analyzed as a first approach to comparing their relative efficiency in inducing peroxidative damage to cell membranes.

2. Materials and methods

2.1. Chemicals

The salts and solvents used were of analytical grade and were used without further purification. Pure AmB was obtained from Squibb France. Millimolar (except in specified cases) AmB stock solution was prepared in dimethylsulfoxide (DMSO). Just before use, the stock solution was diluted 10-fold, by vigorously stirring in pure water (Millipore Milli Q ion exchanger). AmB solutions (heated for 20 min at 70 °C, or unheated) were prepared from these diluted solutions.

2.2. Calculation of concentration of AmB species and spectroscopic measurements

As will be seen (Fig. 1(a)), the absorption spectrum of AmB, which results from the spectroscopic contributions of aggregates formed at high (At) or low temperature (A), and contributions of monomers (M), depends on the percentages of these forms. For an optical path of length 1 cm, absorbances at 322, 339 and 409 nm defined as A_{322}, A_{339} and A_{409}, respectively, are expressed according to the Beer–Lambert formulation as

$$A_{322} = \epsilon_{322}^{At}[At] + \epsilon_{322}^{A}[A] + \epsilon_{322}^{M}[M] \quad (1)$$

$$A_{339} = \epsilon_{339}^{At}[At] + \epsilon_{339}^{A}[A] + \epsilon_{339}^{M}[M] \quad (2)$$

$$A_{409} = \epsilon_{409}^{At}[At] + \epsilon_{409}^{A}[A] + \epsilon_{409}^{M}[M] \quad (3)$$

Assuming that AmB aqueous solutions correspond to a mixture of these three spectroscopic species, the total AmB concentration was expressed as the sum [At] + [A] + [M]. As demonstrated below, the good agreement between the values of the total

AmB concentration estimated in this way and the theoretically expected values supports this hypothesis. Molar extinction coefficients (ϵ) for each spectroscopic species were deduced from their typical absorption spectra at 409, 322 and 339 nm for monomers (spectrum obtained for 10^{-7} M AmB), and for aggregates heated at 70 °C or unheated (spectra obtained for 10^{-4} M AmB). The mean ϵ values reported in Table 1 were obtained from three measurements (standard deviations less than 5%). The superscripts denote aggregated AmB at high (At) or low (A) temperature and for the monomeric form

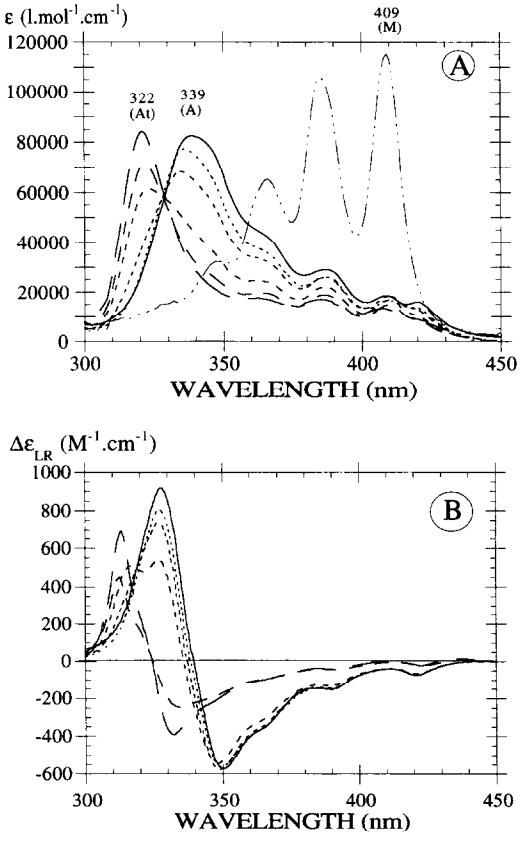

Fig. 1. Heat-induced changes in the AmB aggregation state in aqueous solutions: (a) absorption spectra; (b) circular dichroism spectra. The absorption and CD spectra were obtained at a low concentration (10^{-7} M) for monomers (M; – · · · –) and at a higher concentration (10^{-4} M) for samples heated at $\Theta = 25$ °C (————), $\Theta = 45$ °C (---), $\Theta = 55$ °C (– – –), $\Theta = 57.5$ °C (— — —), $\Theta = 60$ °C (— — — —), $\Theta = 70$ °C (— — — —). The amplitude of the monomer CD spectrum is very low and is not drawn in the figure.

Table 1
Molar extinction coefficients ϵ at 322, 339 and 409 nm of AmB aqueous solutions (prepared from a 10^{-3} M DMSO stock solution) as a function of aggregation state

	ε_{322}	ε_{339}	ε_{409}
At	87200	38800	7100
A	32500	83900	13200
M	11800	20800	115300

The three spectroscopic species were obtained at a low concentration (10^{-7} M) for monomers (M) and at a high concentration (10^{-4} M), with aggregates heated for 20 min at 70 °C (At), or unheated (A). The mean ϵ values were obtained from three measurements (standard deviations less than 5%). For the high concentration (10^{-4} M), the values were corrected for the low contribution of the monomeric form (less than 5%).

(M), while the subscripts indicate the wavelength of the measurement. For high concentrations (10^{-4} M), the ϵ values were corrected for the low contribution of the monomeric form (less than 5%).

The mean number of AmB monomeric units in each aggregated form is unknown and probably corresponds to a wide size distribution. Consequently, the ϵ values were estimated considering monomeric AmB. The concentrations of M, At and A were expressed in terms of monomeric AmB. These concentrations, which are the solutions of Eq. (1)–(3), were calculated according to the expressions

$$\begin{aligned}[M] = \{&[(\epsilon^{A}_{322}A_{409} - \epsilon^{A}_{409}A_{322})\\ &\times(\epsilon^{A}_{322}\epsilon^{At}_{339} - \epsilon^{A}_{339}\epsilon^{At}_{322})]\\ &-[(\epsilon^{A}_{322}A_{339} - \epsilon^{A}_{339}A_{322})\\ &\times(\epsilon^{A}_{322}\epsilon^{At}_{409} - \epsilon^{A}_{409}\epsilon^{At}_{322})]\}\\ &\times\{[(\epsilon^{A}_{322}\epsilon^{M}_{409} - \epsilon^{A}_{409}\epsilon^{M}_{322})\\ &\times(\epsilon^{A}_{322}\epsilon^{At}_{339} - \epsilon^{A}_{339}\epsilon^{At}_{322})]\\ &-[(\epsilon^{A}_{322}\epsilon^{M}_{409} - \epsilon^{A}_{339}\epsilon^{M}_{322})\\ &\times(\epsilon^{A}_{322}\epsilon^{At}_{409} - \epsilon^{A}_{409}\epsilon^{At}_{322})]\}^{-1} \end{aligned} \quad (4)$$

$$\begin{aligned}[A] = [&(\epsilon^{At}_{322}A_{339} - \epsilon^{At}_{339}A_{322})\\ &-[M](\epsilon^{M}_{339}\epsilon^{At}_{322} - \epsilon^{M}_{322}\epsilon^{At}_{339})]\\ &\times[(\epsilon^{A}_{339}\epsilon^{At}_{322} - \epsilon^{A}_{322}\epsilon^{At}_{339})]^{-1} \end{aligned} \quad (5)$$

$$[At] = \frac{A_{322} - [A]\epsilon^{A}_{322} - [M]\epsilon^{M}_{322}}{\epsilon^{At}_{322}} \quad (6)$$

Absorption measurements were performed using a CARY-1E UV–visible spectrophotometer controlled by a personal computer. The temperature was regulated by a thermostat-equipped cuvette holder. The optical path of the quartz cuvettes (0.1, 0.5, 1 and 10 cm in size) was chosen to obtain absorbance values lower than 1.5. After readings at 322, 339 and 409 nm (band width, 4 nm; signal averaging time, 2 s), the concentrations and percentages of each species were calculated according to Eq. (4)–(6). The Rayleigh scattering contribution, which depends on the aggregate size, was simultaneously monitored in a spectral range where AmB does not absorb (650 nm). Except for specified cases, the absorption measurements were performed immediately after preparing the AmB solutions.

Circular dichroism (CD) spectra were recorded with a Jobin–Yvon Mark IV dichrograph using a thermostat-equipped cuvette holder. $\Delta\epsilon$ (M^{-1} cm^{-1}) is the differential molar dichroic absorption coefficient.

3. Results

3.1. Heat-induced changes in the aggregation state of AmB in aqueous solution

AmB self-association in water was previously reported to be concentration dependent [13,29]. For concentrations lower than 10^{-6} M, in aqueous solution, the monomeric form of AmB (M) predominates, with a typical absorption spectrum exhibiting maxima at 365, 384 and 409 nm and a shoulder at around 348 nm (Fig. 1(a)). The CD spectrum of the monomer does not show any significant dichroic doublet.

At higher concentrations, self-association and aggregation occur, leading to changes in the spectroscopic properties. At 10^{-4} M, when practically all the molecules are aggregated (around 95% of A), a bathochromic shift occurs (Fig. 1(a)) with a new maximum at 339 nm. Two minor peaks also appear at 390 and 420 nm. At this concentration, the CD spectrum of AmB (Fig. 1(b)) exhibits a dichroic doublet centered at 339 nm (positive and negative peaks at 329 and 350 nm respectively), indicating an organized asymmetric structure. Such a CD spectrum, which is typical of the self-associated soluble form of AmB, is assumed to reflect excitonic interactions between the AmB molecules within the aggregates [13,24,29].

3.1.1. Effect of heating to 70 °C

Heating (for 20 min at 70 °C) and cooling the concentrated (10^{-4} M) solution leads to significant changes in the AmB aggregation state. The thermal treatment does not induce molecular dispersion but seems to increase the size of aggregates until flocculation occurs. Light scattering by the concentrated AmB solution increases after heating, indicating an increase in aggregate size until flocculation. The opalescent solution obtained is subjected to centrifugation at $12\,000 \times g$ for 10 min to eliminate insoluble aggregates as a yellow precipitate, leading to a clear solution. This increase in aggregate size explains the term 'superaggregate' used in the present study to define the heat-induced aggregation state of AmB. It is possible to detect this heat-induced change in aggregation by analyzing typical changes that occur in the solution spectroscopic properties on heating.

As shown in Fig. 1(a), the absorption at 339 nm of the 10^{-4} M solution in water progressively decreases, while a new peak centered at 322 nm appears when the temperature increases from 25 to 70 °C. An isobestic point around 328 nm, when the temperature increases from 25 to 70°C, suggests that the aggregated species that absorbs at 339 nm (A) was thermally converted to another form that shows a maximum at 322 nm. These two maxima (339 and 322 nm) correspond to pure electronic transitions, as suggested by the first derivative processed spectra. The solution absorption spectrum remained unchanged for temperatures higher than 70 °C with its maximum at 322 nm—which is typical of the new superaggregated form At—one minor absorption peak centered at 420 nm and a shoulder at around 390 nm. A bathochromic shift and a decrease in the intensity of the dichroic doublet can be seen in the CD spectrum of the concentrated solution when the temperature is increased from 25 to 70 °C (Fig. 1(b)). At 70 °C, the new species (At) exhibits a typical CD spectrum centered at 322 nm, with positive and negative peaks at 313 and 332 nm respectively.

3.1.2. Temperature profile and distribution of the species as a function of temperature

The three spectroscopic species (M, A and At) obtained at low concentrations (10^{-7} M) for monomers (M), and at high concentration (10^{-4} M) for heated (At) or unheated (A) aggregates, were present as mixtures between these two concentration limits. The absorption properties of the species, as summarized in Fig. 1(a) and Table 1, were taken as references to process the absorption data at 322, 339 and 409 nm according to the algorithms described above. The concentrations of each spectroscopic species as a function of temperature—calculated according to this algorithm—are shown in Fig. 2(a).

At high concentrations (1.1×10^{-4} M), the monomeric form is negligible, while practically all the AmB molecules are self-associated. The heat-induced transition from the A form to the superaggregated At form occurs slowly up to 50 °C, and occurs faster for temperatures between 50 and 60 °C. The midpoint of the transition occurs at around 56 °C. At 70 °C, practically all the self-associated form A is converted into the At form. As shown in Fig. 2(b), by subtracting the concentration of both forms A + M from the theoretical AmB concentration, we obtain a value similar to the concentration of the superaggregated form At for each temperature below the transition temperature. This result not only provides further validation of the algorithm but also indicates that At formation results from the condensation of the monomeric form M with the aggregated form A.

Light scattering increases on At formation, indicating that this spectroscopic species probably corresponds to an aggregation state higher than that of A. The total AmB concentration calculated from the absorption data remains practically constant up to 50 °C and decreases slightly at higher temperatures. Maintaining the solution at 70 °C for 1 h also leads to a slight decrease in the total AmB concentration, probably as a consequence of the auto-oxidation process that takes place in AmB solutions when the temperature increases (see below).

3.1.3. Dissociation of A aggregates and At superaggregates on dilution

The concentration threshold beyond which the aggregated forms of the AmB derivatives dissociate into monomers is generally assumed to be an important parameter that modulates the biological activities of the derivatives. Progressive dilution of the aggregated form A, as obtained from an unheated 10^{-4} M aqueous solution, leads to its dissociation into the monomeric form (Fig. 3(a)). (The very low percentage of At superaggregates generated under these conditions is not reported in the figure). At 1×10^{-6} M, half of the unheated AmB solution is in the form of A aggregates and the other half is in the monomeric form.

As shown in Fig. 3(a), progressive dilution of the

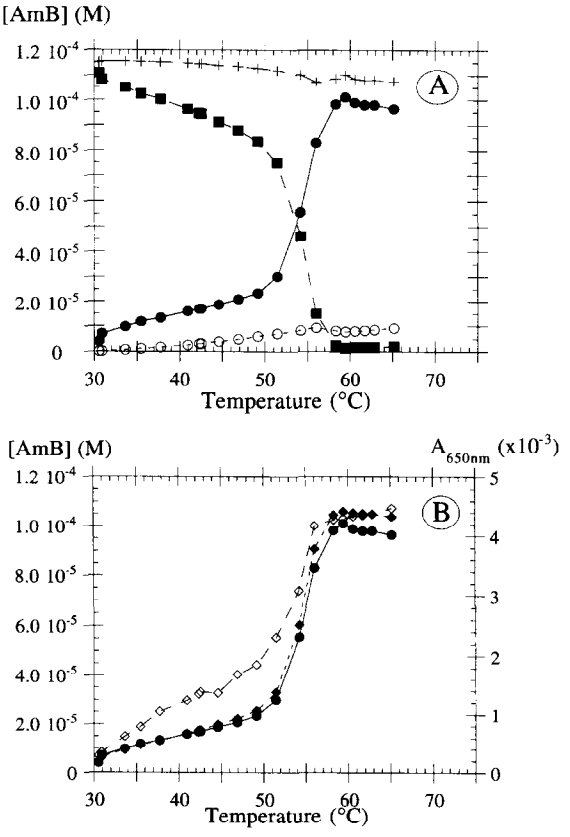

Fig. 2. Heat-induced changes in the AmB (1.1×10^{-4} M) aggregation state in aqueous solutions: (a) concentrations of the spectroscopic species—monomers (M; – ∘ –), heated (At; – · –) or unheated (A; – ■ –) aggregates, and total AmB concentration ([M]+[At]+[A]; – · + · –); (b) heat-induced formation of the superaggregated form At. Left hand scale: (At; – · –), ([AmBtotal]$_{theoretical}$ – [A + M]$_{measured}$; – ◆ –). Right hand scale: scattered light at 650 nm; – ◇ –)Concentrations of the various spectroscopic species were calculated from the absorption data at 322, 339 and 409 nm according to the algorithm described in Section 2.

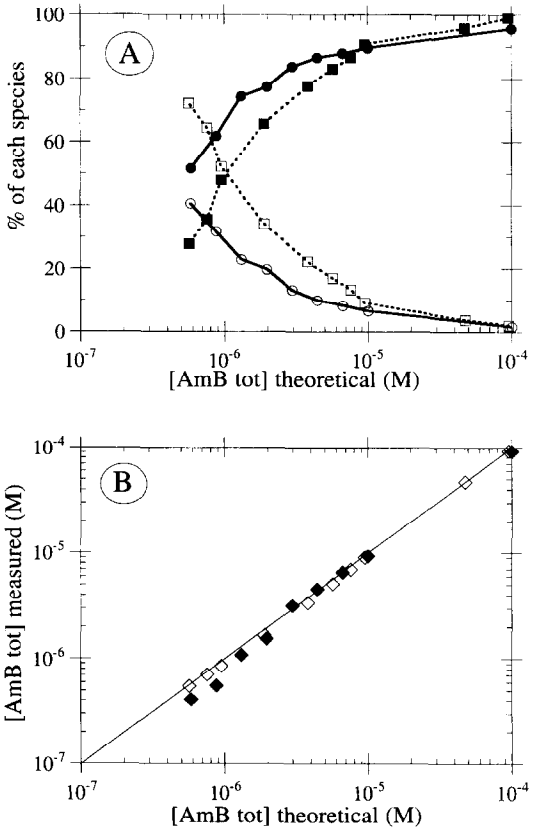

Fig. 3. Distribution of the aggregated species (A and At) and of the monomeric AmB (M) as a function of the concentration. The percentages of the various spectroscopic species were calculated from the absorption data at 322, 339 and 409 nm according to the algorithm described in Section 2. (a) AmB aqueous solutions (10^{-4} M prepared from a 10^{-3} M DMSO stock solution) were successively diluted in water. The solutions were unheated (percentage of A (· · · ■ · · ·) and percentage of M (· · · □ · · ·)) or heated for 20 min at 70°C prior to dilution (percentage of At (– · –) and percentage of M (– ○ –)). (b) Calculated total AmB concentration ([M]+[At]+[A]) as a function of the total AmB concentration (theoretical, ————) expected from the dilution factor. The AmB solutions were unheated (◇) and heated for 20 min at 70°C (◆).

superaggregated form At (10^{-4} M AmB aqueous solution) obtained on heating (20 min at 70°C) also leads to the dissociation of the superaggregate into monomers. Data were recorded and processed immediately after the dilution at room temperature. The minor aggregated form A, which is only slightly involved in this equilibrium (less than 3%), is omitted from the figure. The 500-fold diluted solution corresponds to a theoretical AmB concentration of 2×10^{-7} M and exhibits an absorption spectrum close to that typical of the pure monomer (data not shown). The total AmB concentration that leads to 'half-dissociation' (50% monomer and 50% superaggregates) is around 5×10^{-7} M. These data show that the dissociation of the At superaggregates takes place at lower AmB concentrations than is the case for the A aggregates.

Values of the total AmB concentrations ([At] + [A] + [M]) calculated for each dilution as described above are reported in Fig. 3(b) as a function of the total theoretical AmB concentration (expected from the dilution factor). The linear relationship between these two parameters for concentrations higher than 2×10^{-6} M (slope equals 1) provides further validation of the algorithm. In contrast, the underestimation of the calculated values with respect to the theoretical values for concentrations lower than 2×10^{-6} M points to the limit of accuracy of our method and to its range of reliability. This inaccuracy could arise because the processing of data does not include the screening effect that occurs at high concentrations and because of the contribution of light scattering in the heated samples.

3.2. Effect of time and stock solution concentration on the aggregation state of AmB at room temperature

At high concentrations (10^{-5}–10^{-4} M), AmB solutions spontaneously undergo—even at room temperature—slow changes in their spectroscopic properties that reflect changes in the aggregation state. When a 10^{-5} M AmB solution is maintained at 20°C for a long time (100 h), a slight bathochromic shift of the absorption maximum takes place from 339 to 334 nm, while the total AmB concentration decreases by less than 10%. The rate of this spontaneous process can be accelerated by stirring and by decreasing the concentration of the stock solution.

As shown in Fig. 4(a), half of the 1.2×10^{-5} M AmB aqueous solution prepared from a low concentration DMSO stock solution (10^{-4} M) is in the monomeric form and the other half is aggregated (At and A). The spontaneous change in the aggregation state that occurs on stirring as a function of time at 20°C leads to the formation of the aggregated form

At, accompanied by the disappearance of both the A and M forms. During such a conversion from A to At, the total AmB concentration remains practically unchanged (degradation of less than 5%). Over longer periods (100 h), the absorption maximum of this solution, which is typical of the main superaggregated form At (around 322 nm), does not change, while the total AmB concentration decreases by 30% (data not shown).

The proportion of DMSO was kept constant in all the experiments shown in Fig. 4, to avoid changes in the critical micellar concentration. The increase in the DMSO proportion from 1% to 12% was found to increase the amount of the monomeric form and to reduce the amount of the aggregated form A, but it did not induce the formation of the At aggregates (data not shown). As shown in Fig. 4(b), an increase in the concentration of the AmB stock solution (10^{-3} M) gives rise to a higher concentration of A and to a lower monomer concentration. Under these conditions, the concentration of At is negligible just after the dilution, and slowly increases up to 1×10^{-6} M after 20 min of stirring at 20 °C. Over a longer period (100 h), the absorption maximum of this solution, which is typical of the main aggregated form A, is progressively shifted from 340 to 330 nm, while a 60% decrease in the total AmB concentration takes place.

These results clearly show that the change in the AmB aggregation state occurs spontaneously in solutions at room temperature. The results highlight the importance of the method of preparing the diluted solutions. Both the time factor and the concentration of the monomeric form, which is strongly increased in the case of low concentration stock solutions, affect the aggregation process.

Values of the At, A and M concentrations measured for 1.2×10^{-5} M AmB solutions prepared from various DMSO stock solutions after 20 min of stirring at 20 °C are reported in Fig. 4(c). For all the stock solutions between 10^{-4}–10^{-2} M, the monomer concentration reaches equilibrium at a constant value

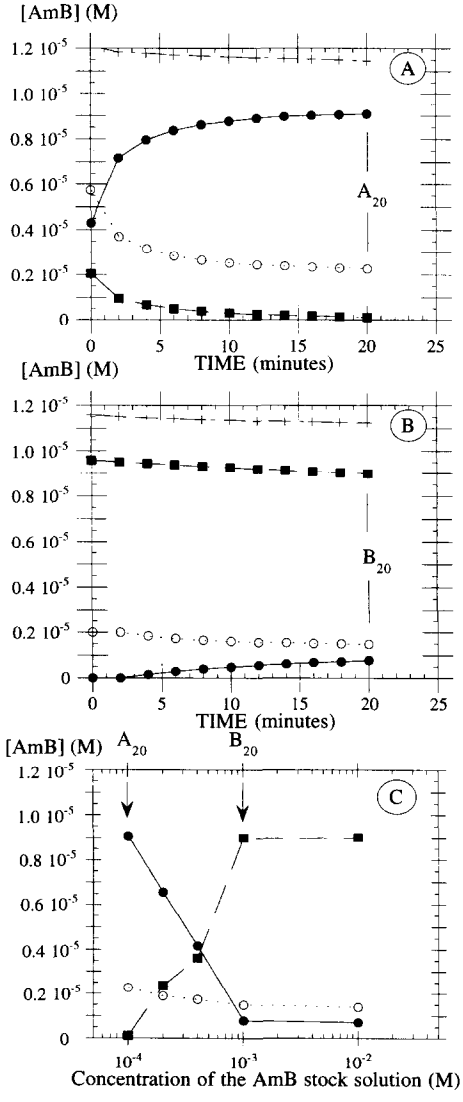

Fig. 4. Kinetics of the spontaneous change in the AmB (1.2×10^{-5} M) aggregation state in aqueous solutions at 20 °C with stirring, showing the monomer (M; – ∘ –), aggregated (A; – ■ –) and superaggregated (At; – • –) forms, and total AmB concentration ([M]+[At]+[A]; – · + · –): (a) AmB solution prepared from a 10^{-4} M DMSO stock solution; (b) AmB solution prepared from a 10^{-3} M DMSO stock solution; (c) concentration of the various spectroscopic species in equimolar (1.2×10^{-5} M) AmB solutions. The percentages of the various spectroscopic species were calculated from the absorption data at 322, 339 and 409 nm according to the algorithm described in Section 2. The figure shows the monomer (M; – ∘ –), aggregated (A; – ■ –) and superaggregated (At; – • –) forms as a function of the concentration of the DMSO stock solution. The proportion of DMSO (12%) was kept constant in all the measurements. A_{20} and B_{20} correspond to the values presented in (a) and (b), respectively, after 20 min of stirring at 20 °C.

close to 2×10^{-6} M. In contrast, the concentrations of the aggregated forms A and At vary greatly under these conditions. Only the superaggregated form At is formed when the concentration of the stock solution is low (10^{-4} M; A_{20}), while the other aggregate A largely predominates for stock solutions of higher concentrations (10^{-3} M; B_{20}). Further evidence for the formation of larger aggregates from lower stock solution concentrations (10^{-4} M) was provided by the threefold increase in light scattering at 650 nm with respect to that observed for solutions prepared from less diluted stock solutions (10^{-3} M).

3.3. Effect of heat treatment on the chemical stability of AmB in aqueous solutions

The stability of the various species was monitored for the experimental conditions used for treatment of biological material. Absorption spectra were recorded for aqueous AmB solutions (10^{-5} M) that were unheated (Fig. 5(a)) or preheated for 20 min at 70 °C (Fig. 5(b)), covering various incubation times at 37 °C, under vigourous stirring. The concentrations of each species calculated from absorption data are reported inset in Fig. 5. The total AmB concentrations estimated using this spectroscopic method are in close agreement with the values obtained using high performance liquid chromatography (data not shown). The decrease in the AmB concentration estimated from spectroscopic and chromatographic analyses depends on various experimental factors, including the temperature, shaking and the oxygen concentration.

Deaerated AmB solutions remain quite stable when kept under nitrogen. As previously reported [27], this result shows that the decrease in the AmB concentration is an oxygen-dependent process and corresponds to the auto-oxidation of the AmB. While the total AmB concentration of the unheated solution shows a 25% decrease after 2 h of incubation (Fig. 5(a)), the AmB auto-oxidation involves less than 10% of the heated solution (Fig. 5(b)). The concentration of the aggregated form A (λ_{max} = 339 nm), as derived from the data in Fig. 5(a), decreases by 40% after 2 h of incubation. About 10% of this decrease results from the condensation of A with M to give the At superaggregate. Fig. 5(b) shows that a decrease of less than 10% occurs after 2 h when the At

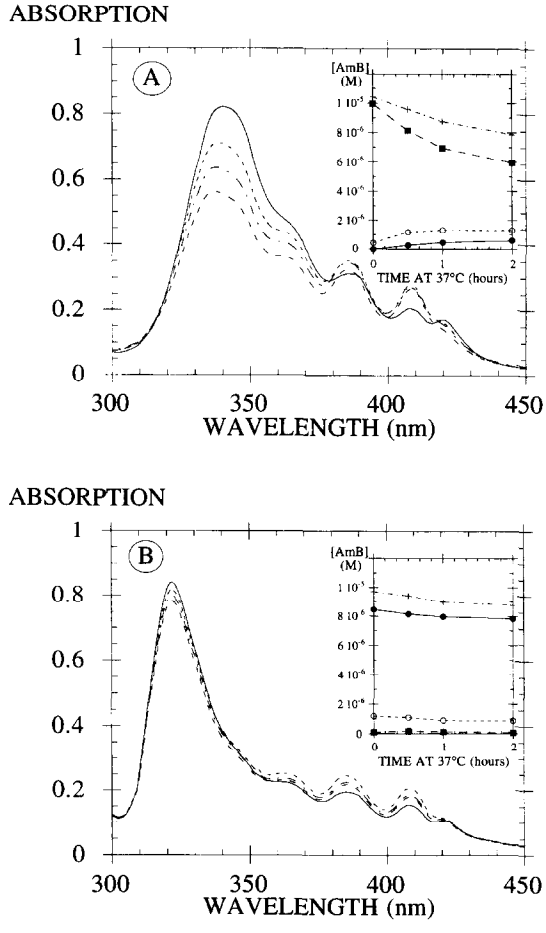

Fig. 5. Effect of thermal pretreatment of the 1×10^{-5} M AmB aqueous solutions on the kinetics of auto-oxidation at 37 °C with stirring: (a) unheated; (b) heat treated (20 min at 70°C). The absorption spectra are shown at 0 min (————), 30 min (- - -), 60 min (-●-●) and 120 min (– – –). Concentrations of the various spectroscopic species reported as insets were calculated from the absorption data at 322, 339 and 409 nm according to the algorithm described in Section 2. The figure shows the monomer (M; – ∘ –), aggregated (A; – ■ –) and superaggregated (At; – · –) forms, and total AmB concentration ([M]+[At]+[A]; – · + · –).

superaggregates are the predominant species (λ_{max} = 322 nm), as obtained after heating for 20 min at 70 °C.

In Fig. 6, we compare the auto-oxidation rate of AmB (for incubation for 2 h) with the concentration of A aggregates obtained with increasing AmB concentration. This rate, expressed as the total amount

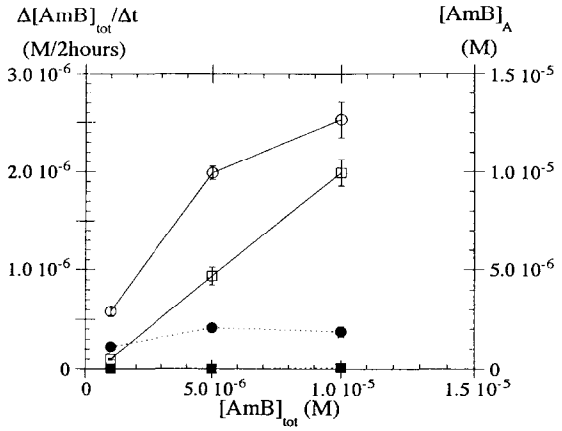

Fig. 6. Involvement of the aggregated species A in the auto-oxidation process of AmB in aqueous solutions at various concentrations. Left-hand scale: total auto-oxidized AmB concentration after 2 h at 37 °C, with the solutions unheated (– ∘ –) or preheated for 20 min at 70 °C (– · –). Right-hand scale: concentration of the aggregated species A calculated from the absorption data at 322, 339 and 409 nm according to the algorithm described in Section 2, with the solutions unheated (– □ –) or preheated for 20 min at 70 °C (– ■ –). Data are the mean values (±SD) of three measurements.

of AmB auto-oxidized after 2 h, increases (left-hand scale) with the concentration of A aggregates (right-hand scale). The auto-oxidation process involves about 50% of the total amount of AmB for a concentration of 1×10^{-6} M, while it reaches no more than 25% for the higher concentration of 1×10^{-5} M. The auto-oxidation rate is low and does not vary significantly with the concentration of solutions heated for 20 min at 70 °C, showing that the concentration of A is very low. As mentioned above, for long stirring times of the 10^{-5} M solutions (obtained from 10^{-3} M DMSO stock solution), these results clearly demonstrate that the chemical stability of At is higher than that of A when incubated under stirring for 2 h at 37 °C, as is the case in our biological assays.

4. Discussion

The self-associated water-soluble form of AmB was previously shown to trigger permeability changes in red blood cell (RBC) membranes [12] and to induce cytotoxic events. In aqueous solutions, characteristic changes in the absorption and CD spectra were reported for concentrations higher than 10^{-7} M. These changes were shown to result from a large spread of aggregated asymmetric structures from dimers to high molecular weight polymers. In human erythrocytes, the higher toxicity of the water-soluble aggregated form with respect to the water-insoluble aggregates was demonstrated after their separation by centrifugation [12]. The concentration threshold beyond which the drug gives rise to aggregates seems to be the main parameter that modulates the biological activity of the drug. In fact, AmB derivatives with a higher concentration threshold for aggregation are less efficient for inducing RBC permeability (preliminary results).

In the present study, changes in the absorption properties of AmB related to its aggregation state were analyzed to estimate the quantities of each spectroscopic species in equilibrium in aqueous solution. Heat treatment was shown to modify the aggregation state of the AmB. The spectroscopic species At, generated after heating ($\lambda_{abs}^{max} = 322$ nm, Fig. 1(a)), exhibits a dichroic doublet in its CD spectrum that is typical of an aggregated state that displays excitonic interactions between monomeric units. The At form results from condensation of the aggregated form A ($\lambda_{abs}^{max} = 339$ nm) with monomers ($\lambda_{abs}^{max} = 409$ nm), and probably corresponds to a superaggregated state with a size larger than that of A, as inferred from the significant increase in light scattering after thermal treatment. This increase was concomitant with the formation of At as well as with the disappearance of both A and M. Furthermore, the opalescence that results from the superaggregates in the heated solutions was removed by centrifugation (12 000 g for 10 min).

When formed, the superaggregated state At was shown to be in equilibrium with the monomeric form, independently of the other aggregated form A. The dissociation of At superaggregates into monomers takes place at lower AmB concentrations than is the case for the A aggregates.

A thermally induced increase in aggregate size in Fungizone® aqueous solutions (10^{-5} M) has been reported [24]. The size, as deduced from light scattering measurements, was constant until 60 °C and increased rapidly at higher temperatures. In aqueous solution at 70 °C, the apparent mass of the aggregates

was shown to be about 500-fold larger than the mass at 20 °C, so justifying the term 'superaggregate' used in the present study.

At low concentrations (less than 2×10^{-6} M), AmB induces a reversible permeabilizing effect on erythrocytes, while it causes lysis at higher concentrations. The relationship between these two distinct mechanisms of action is neither generally admitted nor clearly elucidated. However, it is generally assumed that permeabilizing effects are related to AmB's ability to form transmembrane channels, while the lytic effect could be caused by its peroxidative action at the membrane level [26]. The oxidation of unsaturated fatty acids leads to a fragilization of the membrane, which becomes more sensitive to leakage-induced osmotic shock, as a result of the channel formation.

Auto-oxidation of AmB in solution, as well as AmB-induced peroxidation of unsaturated acyl chains of cell membranes have been assumed to be triggered by reactive oxygen species produced by the antibiotic [28]. Free radical formation during Fungizone® auto-oxidation was previously demonstrated by following the kinetics of decay of the electron spin resonance (ESR) signal of TEMPOL—a stable nitroxide [27,28]. The restricted mobility of these radicals suggests that they arise from AmB molecules in aggregates. Our present comparison of the stabilities of various AmB aggregation states strongly supports this assumption.

The monomeric form of AmB is not involved in the auto-oxidation process. Furthermore, greater stability of the heat-treated samples (mainly At) with respect to the unheated samples (mainly A) was observed in our study. This result suggests that At is less efficient than is the A form for producing reactive oxygen species. The auto-oxidation rate of A is probably the limiting step of its degradation process. This would explain why the increase in the amount of auto-oxidized AmB is not proportional to the increase in the concentration of A and, consequently, why the percentage of A that undergoes auto-oxidation decreases with increasing AmB concentration. With regard to the peroxidative and lytic actions of AmB, the above considerations could also explain the lower lytic efficiency of the heat-treated samples (in preparation).

Temperature (in the range 10–40 °C) was previously reported to modulate AmB's ability to induce K^+ leakage from large (cholesterol-containing) unilamellar vesicles (LUVs) [10]. The decrease in the intensity of the CD doublet centered at around 340 nm, which is characteristic of the aggregated species (A form in the present work), was interpreted in the previous study as a decrease in the AmB aggregation state. Consequently, the heat-induced decrease in the AmB permeabilizing effect was assigned to molecular dispersion of the aggregates. The present results allow us to conclude that superaggregation processes occur at a slow rate at 40 °C, as indicated by absorption and CD data, as well as by light scattering measurements (Fig. 2). The results underline that a decrease in the CD doublet could also be related to a blue-shift of the electronic transition and/or to the appearance of a weak CD doublet at lower wavelength—both events reflect an increase in aggregate size.

Our results show that spontaneous changes in the aggregation state also occur in aqueous AmB solutions (10^{-4}–10^{-5} M) maintained at 20 °C, leading to the formation of the superaggregated form At. During thermal conversion, this spontaneous aggregation that takes place at room temperature is related to the concomitant disappearance of both forms A and M, and is responsible for a relative increase in the aggregate size, as suggested by light scattering measurements. In contrast to the thermally induced aggregation, the rate of the spontaneous process at 20 °C is slow and depends on the monomer concentration.

For a constant AmB concentration (10^{-5} M), a low concentration of the DMSO stock solution (10^{-4} M) leads to a relatively high percentage of monomer in the diluted solution, so increasing the rate of spontaneous At formation by condensation of A with M. In contrast, this rate is greatly decreased in equimolar solutions prepared from higher concentration stock solutions (10^{-3} M), so leading to large amounts of A. In this second case, the slow transition between the aggregated state (A, 339 nm) and the superaggregated state (At, 322 nm) is not characterized by an equilibrium between both species, as suggested by the absence of an isobestic point. For long periods (10–100 h), the formation of superaggregates seems to involve intermediate aggregation states, each showing typical spectroscopic properties,

as suggested by the progressive blue-shift of both the absorption maximum and the processed absorption data as first derivative.

In a previous study [12], the kinetics of AmB-induced K^+ leakage from human RBCs was shown to depend on the concentration of the stock solution; the kinetics were slower for concentrated DMSO or dimethylsulfoxide (DMF) stock solutions (10^{-2} M). The insoluble self-associated form (high molecular weight) that was separated by centrifugation was concluded to be less permeabilizing at 2×10^{-6} M. While our study provides qualitative information that is in agreement with this work, a direct, quantitative comparison between these results and the present data is not possible, because the various species were not similarly defined in both studies. We describe here spectroscopic properties of the various aggregated species, while Legrand et al. [12] discriminate between these species on the basis of size. Finally, our present results provide a plausible interpretation of the blue-shift of the dichroic doublet observed on decreasing the concentration of the DMSO stock solution in the previous work .

Ernst et al. studied AmB–DOC aggregates in aqueous solutions by measuring changes in the optical spectra as a function of the AmB and ethanol concentrations [11], as well as the variation with temperature [24]. When the temperature increased, the authors observed a weakening of the excitonic CD, an increase in the monomer absorption and a slight blue-shift (at around 7 nm) of the 328 nm absorption peak as a result of the aggregates—associated with an increase in aggregate size—as detected by Rayleigh scattering. The absorption and CD spectra of the AmB aggregates exhibit features that strongly suggest that they are linear polymers. It is generally assumed that the simplest polymer in agreement with these spectroscopic properties is a helix with dimers as elementary units [3,11]. In this model, the hydrophobic side of the AmB molecule, i.e. the polyene moiety, is protected from the aqueous environment. When the temperature rises, the frequency of hydrophobic interactions is assumed to increase, resulting in a blue-shift of the absorption maximum. These new spectroscopic species have been demonstrated to be more stable than the aggregates observed at room temperature.

In the present study, we demonstrated that the formation of superaggregates, which seems to result from the condensation of A aggregates with the monomer, is a slow process at room temperature. Heating can cause an increase in the monomer concentration and/or in the hydrophobic forces, leading to an increase in the condensation rate. In this case, the blue-shift observed in the absorption maximum could result from the higher stacking in the superaggregates, and their relative chemical stability could reflect the low exposure of the polyenic structure to the aqueous solvent.

5. Conclusions

In the present study, we have demonstrated changes in the aggregation state of AmB in solution after heating at 50–60 °C. The concentrations of aggregates formed at high (At) or room (A) temperature, and that of monomeric AmB (M) were calculated by processing absorption data. The thermally induced conversion of A to At depends on the AmB concentration. Rayleigh scattering measurements suggest that At aggregates are larger than A. The At superaggregates were shown to be in equilibrium with the monomers. Their dissociation into monomers takes place at lower AmB concentrations than those observed for the A aggregates.

At room temperature, the A–M condensation rate that leads to the At superaggregate is slower than the corresponding rate at 70 °C, and seems to depend on the monomer concentration. These results clearly show that the change in the AmB aggregation state occurs slowly in solution at room temperature. The results indicate the importance of the method of preparation of the diluted solutions. Both time and the concentration of the stock solution affect the aggregation.

The At superaggregate and the monomer are more stable than the aggregated species A. The auto-oxidation process involves mainly the aggregated A form, which was previously demonstrated to be more efficient at inducing K^+ leakage and lysis in RBCs.

These results show that the superaggregated form At generated by heating at 70 °C or by diluting the stock solution at room temperature constitutes an AmB monomer reservoir. The relative stability of this species probably reflects its low efficiency for

auto-oxidizing via the formation of reactive radical species. Assuming that the toxicity of AmB is mainly related to its aggregation (A form), these physicochemical properties of the superaggregated form At suggest that this species could be less toxic to mammalian cells. We are currently investigating the biological properties of the heat-induced superaggregated form of Fungizone® in RBCs, cultured human cells and fungal cells. Our preliminary data confirm that heat treatment of Fungizone® solutions at 70 °C for 20 min could provide a new solution for the simultaneous improvement of the therapeutic efficiency of AmB against fungal cells and the reduction of its cytotoxicity to mammalian cells (in preparation).

Acknowledgements

The authors are grateful to one of the referees for his constructive remarks.

References

[1] J. Bolard, Biochim. Biophys. Acta, 864 (1986) 257.
[2] J. Brajtburg, W.G. Powderly, G.S. Kobayashi and G. Medoff, Antimicrob. Agents Chemo., 34 (1990) 381.
[3] R.P. Hemenger, T. Kaplan and L.J. Gray, Biopolymers, 22 (1983) 911.
[4] J. Mazerski, J. Grzybowska and E. Borowski, Euro. Biophys. J., 18 (1990) 1.
[5] J. Barwicz, S. Christian and I. Gruda, Antimicrob. Agents Chemo., 36 (1992) 2310.
[6] J. Barwicz, W.I. Gruszecki and I. Gruda, J. Colloid Interface Sci., 158 (1993) 71.
[7] M.T. Lamy-Freund, V.F.N. Ferreira and S. Schreier, Biochim. Biophys. Acta, 981 (1989) 207.
[8] M.T. Lamy-Freund, S. Schreier, R.M. Peitzsch and W.F. Wayne, J. Pharmaceut. Sci., 80 (1991) 262.
[9] A.R. Balakrishnan and K.R.K. Easwaran, Biochim. Biophys. Acta, 1148 (1993) 269.
[10] H.E. Lambing, B.D. Wolf and S.C. Hartsel, Biochim. Biophys. Acta, 1152 (1993) 185.
[11] C. Ernst, J. Grange, H. Rinnert, G. Dupont and J. Lematre, Biopolymers, 20 (1981) 1575.
[12] P. Legrand, E.A. Romero, B.E. Cohen and J. Bolard, Antimicrob. Agents Chemo., 36 (1992) 2518.
[13] J. Bolard, P. Legrand, F. Heitz and B. Cybulska, Biochemistry, 30 (1991) 5707.
[14] R. Jankneght, S. Marie, I.A.J.M. Baker-Wondenberg and D.J.A. Crommelin, Clin. Pharmacokin., 23 (1992) 279.
[15] G. Lopez-Berestein, G.P. Bodey, V. Fainstein, M. Keating, L.S. Frankel, B. Zeluff, L. Gentry and K. Mehta, Arch. Internal Med., 149 (1989) 2533.
[16] F.C. Szoka, Jr., and M. Tang, J. Liposome Res., 3 (1993) 363.
[17] J. Bolard, V. Joly and P. Yéni, J. Liposome Res., 3 (1993) 409.
[18] J.P. Adler-Moore and R.T. Proffitt, J. Liposome Res., 3 (1993) 429.
[19] A.S. Janoff, W.R. Perkins, S.L. Saletan and C.E. Swenson, J. Liposome Res., 3 (1993) 451.
[20] L.S.S. Guo and P.K. Working, J. Liposome Res., 3 (1993) 473.
[21] S.C. Hartsel, S.K. Benz, W. Ayenew and J. Bolard, Euro. Biophys. J., 23 (1994) 125.
[22] J.E. Bennett, G.J. Hill, W.T. Butler and C.W. Emmons, Antimicrob. Agents Chemo. (1963) 745.
[23] F. Bernaudin, J. Hathorn, R. Schaufele and P.A. Pizzo, Pathol. Biol., 35 (1987) 1403.
[24] C. Ernst, G. Dupont, H. Rinnert and J. Lematre, C.R. Acad. Sci. Paris, 286 (1978) 175.
[25] M.T. Lamy-Freund, V.F.N. Ferreira and S. Schreier, J. Antibiot., 38 (1985) 753.
[26] J. Brajtburg, S. Elberg, D.R. Schwartz, A. Vertut-Croquin, D. Schlessinger, G.S. Kobayashi and G. Medoff, Antimicrob. Agents Chemo., 27 (1985) 172.
[27] S. Schreier and M.T. Lamy-Freund, Quim. Nova, 16 (1993) 343.
[28] M.T. Lamy-Freund, V.F.N. Ferreira, A. Faljoni-Alario and S. Schreier, J. Pharmaceut. Sci., 82 (1993) 162.
[29] J. Bolard, M. Seigneuret and G. Boudet, Biochim. Biophys. Acta, 599 (1980) 280.